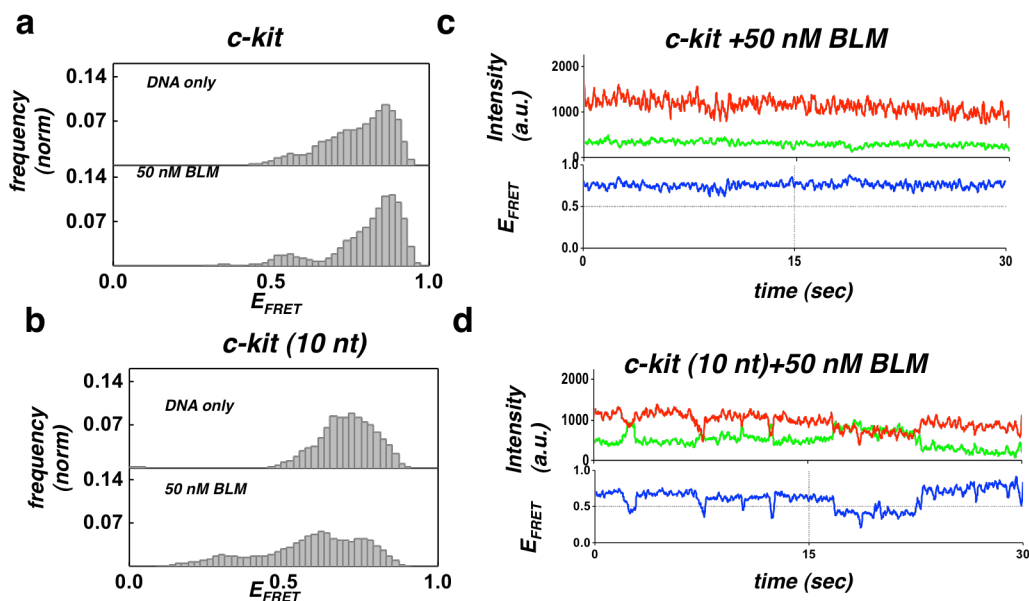


Supplementary Figure 1. Formation of G4 with titration of K, and behavior of G4 (5 nt) substrate in the presence of BLM.

(a) Illustrations of DNA substrates used in this study: (1) Regular G4 substrate. (2) G4 (5 nt) substrate. (3) G4 (10 nt) substrate. (4) Regular 30 nt tailed substrate. (5) Short 10 nt tailed substrate. (6) Gapped substrate with 10 nt gap. (7) Hairpin substrate. (b) Quantification of G4 folded population as a function of KCl. G4 folded population was calculated from the FRET histograms as the percent population at high FRET (>0.6). (c) Representative smFRET trajectory of the G4 substrate in the absence of salt in the buffer showing predominantly low FRET indicating that the G4 structure is unfolded



Supplementary Figure 2. Substrate specific interaction of BLM with G4-forming human c-kit2 sequence.

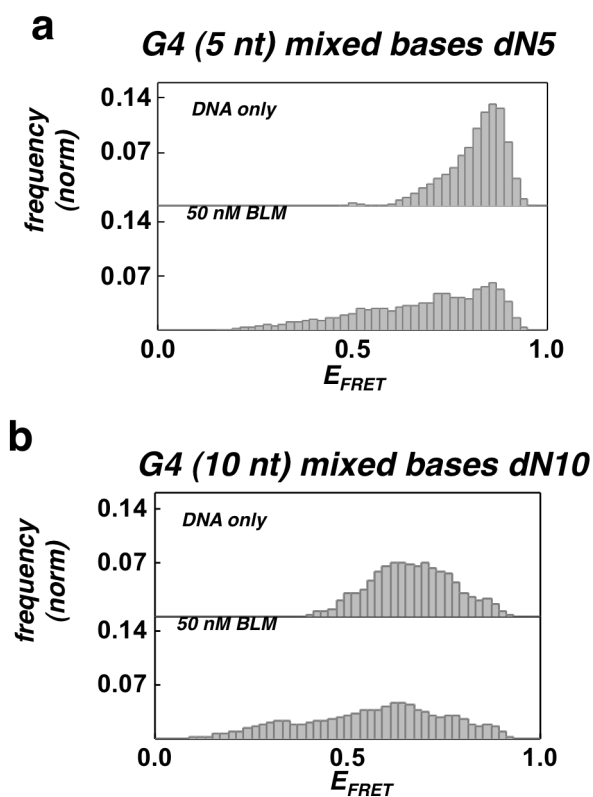
(a) FRET histograms for the c-kit2 G4 substrate, with G4 motif immediately adjacent to duplex region. No change in FRET distribution was observed following addition of 50 nM of BLM (bottom panel).

(b) FRET histograms for the c-kit2 G4 (10nt) substrate with a 10 nt ssDNA between the G4 motif and duplex region. A substantial change in the FRET distribution was detected upon addition of 50 nM BLM (bottom panel).

Histograms in (a) and (b) were generated after subtracting the zero FRET values and truncating the photo bleached part from FRET trajectory. A minimum of 100 smFRET trajectories was used to generate the histograms. The concentration of K^+ was kept at 50 mM

(c) A representative single molecule trajectory of the c-kit2 G4 substrate in the presence of 50 nM BLM showing persistent high FRET. Top panel: donor (green) - acceptor (red) intensities, bottom panel: corresponding FRET trajectory.

(d) Representative smFRET trajectory of the c-kit2 G4 (10nt) substrate in the presence of 50 nM BLM showing dynamic fluctuations in FRET signal (blue).

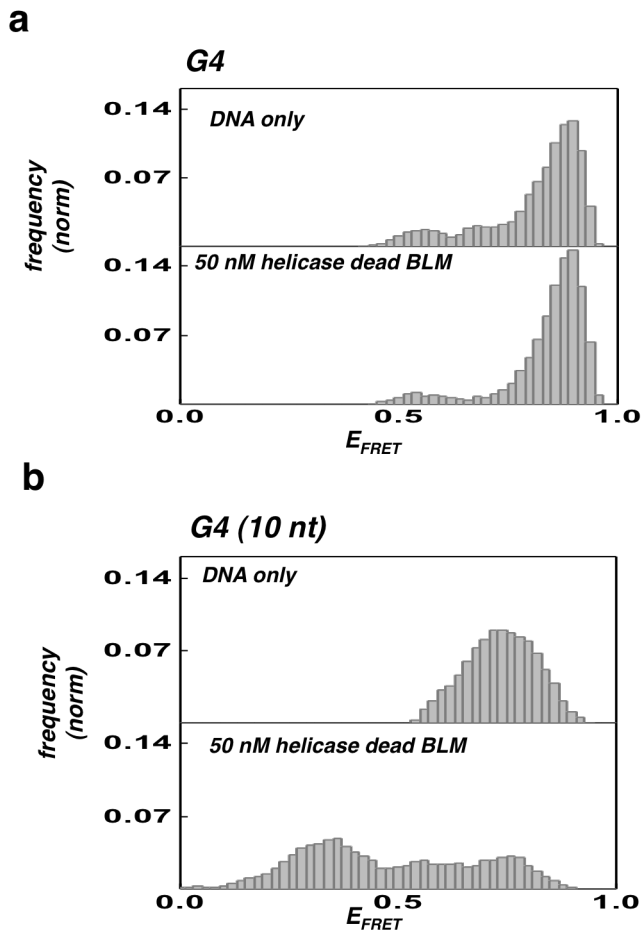


Supplementary Figure 3. Substrate specific interaction of BLM with G4-forming human telomere sequence for mixed ssDNA spacer.

(a) FRET histograms for the G4 (5nt) substrate with a mixed sequence of 5 nt ssDNA between the G4 motif and duplex region. A change in the FRET distribution was detected upon addition of 50 nM BLM (bottom panel).

(b) FRET histograms for the G4 (10nt) substrate with a mixed sequence of 10 nt ssDNA between the G4 motif and duplex region. A substantial change in the FRET distribution was detected upon addition of 50 nM BLM (bottom panel).

Histograms were generated after subtracting the zero FRET values and truncating the photo bleached part from FRET trajectory. A minimum of 100 smFRET trajectories was used to generate the histograms. The concentration of K^+ was kept at 50 mM

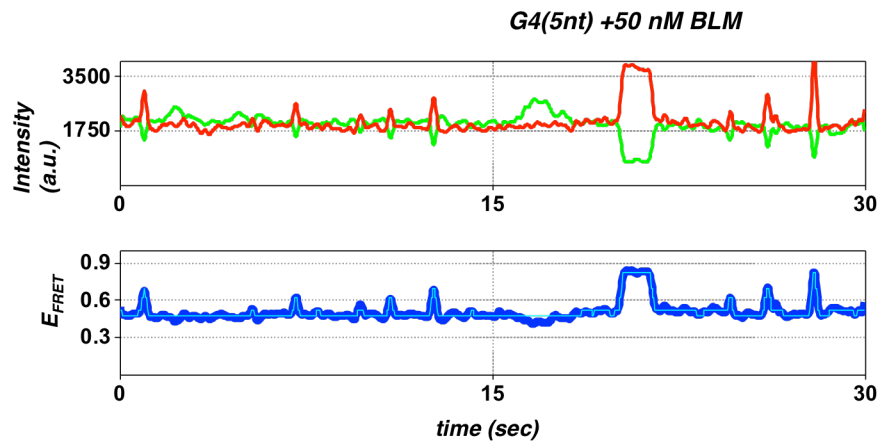


Supplementary Figure 4. Substrate specific interaction of helicase dead BLM with G4-forming human telomere sequence.

(a) FRET histograms for the G4 substrate, with G4 motif immediately adjacent to duplex region. No change in FRET distribution was observed following addition of 50 nM of BLM (bottom panel).

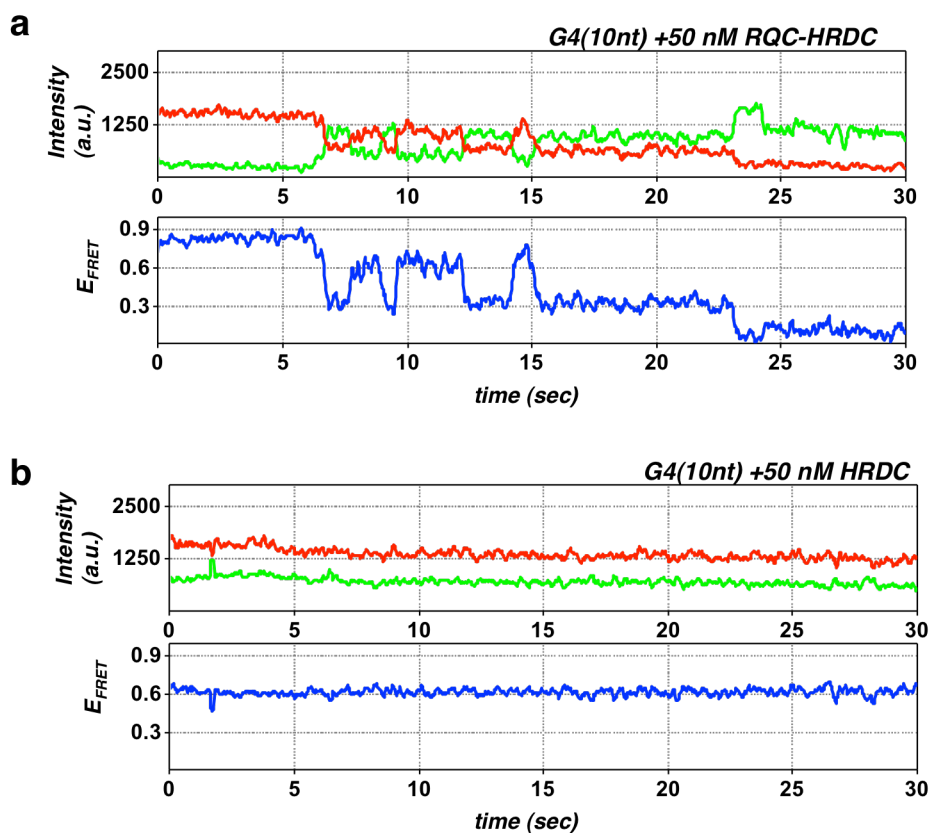
(b) FRET histograms for the G4 (10nt) substrate with a 10 nt ssDNA between the G4 motif and duplex region. A substantial change in the FRET distribution was detected upon addition of 50 nM BLM (bottom panel).

Histograms were generated after subtracting the zero FRET values and truncating the photobleached part from FRET trajectory. A minimum of 100 smFRET trajectories was used to generate the histograms. The concentration of K^+ was kept at 50 mM



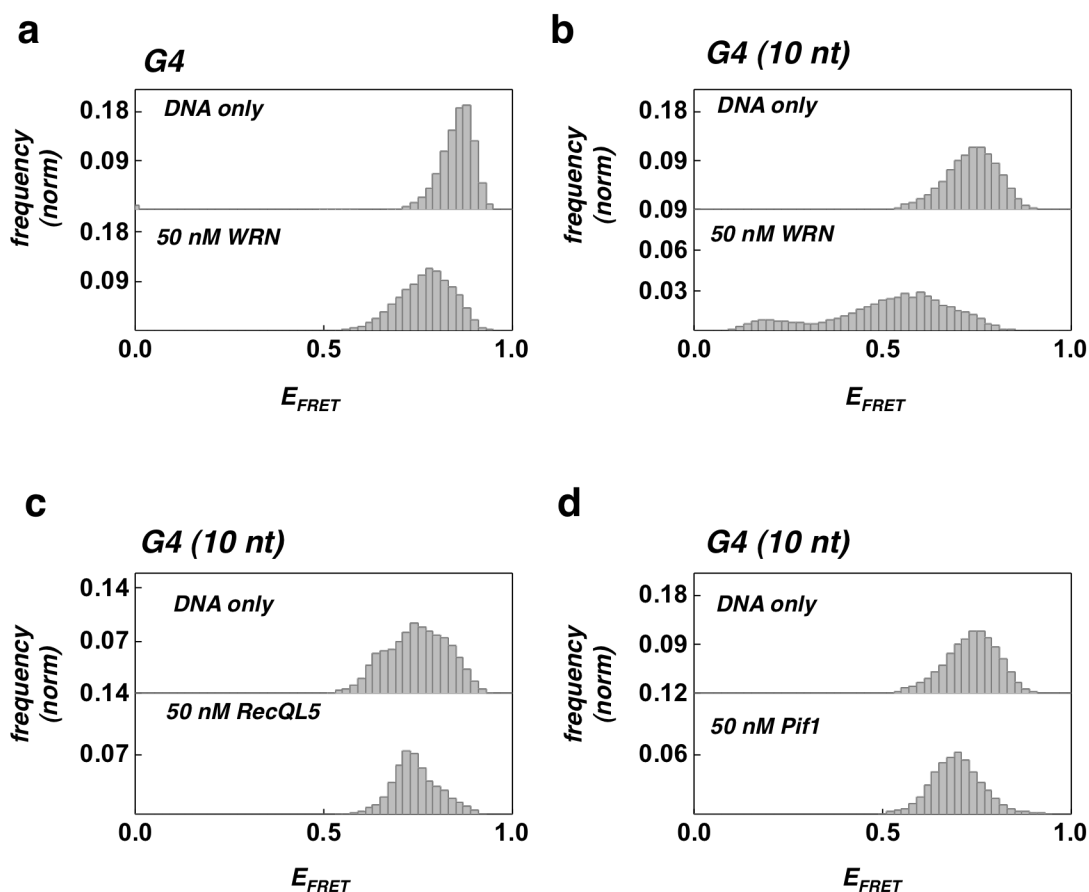
Supplementary Figure 5. smFRET trajectory of G4(5nt) substrate in the presence of BLM.

Representative smFRET trajectory of the G4 (5nt) substrate in the presence of 50 nM BLM showing dynamic fluctuations in FRET. The FRET signal in the bottom curve is in blue whereas the HMM fit is in Cyan.



Supplementary Figure 6. smFRET trajectories of G4(10nt) substrate in the presence of RQC-HRDC and HRDC truncation mutants.

Representative smFRET trajectory of the G4 (10nt) substrate in the presence of (a) 50 nM RQC-HRDC showing dynamic fluctuations in FRET. (b) 50 nM HRDC showing persistent FRET signal.



Supplementary Figure 7. Substrate specific interaction of WRN, RecQL5 and Pif1 helicases with G4-forming human telomere sequence.

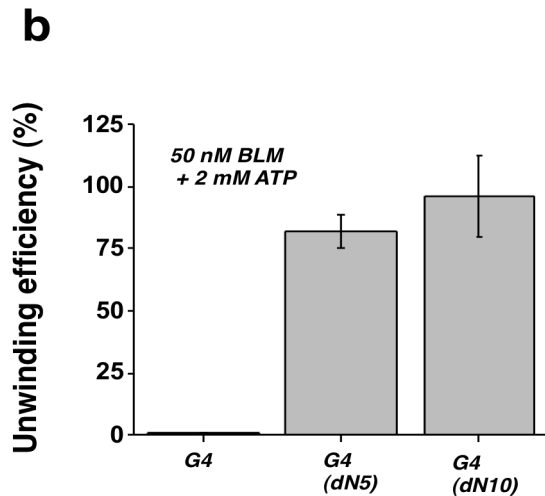
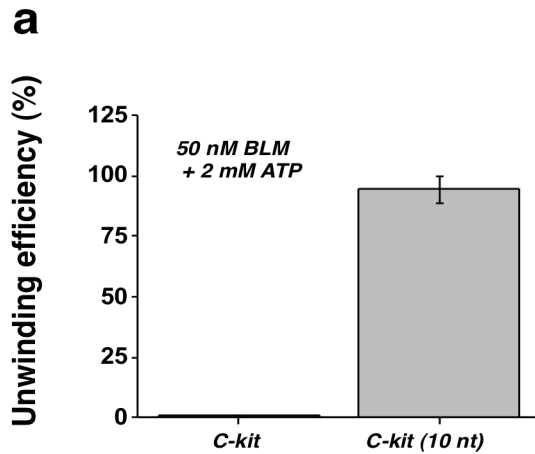
(a) FRET histograms for the G4 substrate, with G4 motif immediately adjacent to duplex region. No change in FRET distribution was observed following addition of 50 nM of WRN (bottom panel).

(b) FRET histograms for the G4 (10nt) substrate with a 10 nt ssDNA between the G4 motif and duplex region. A substantial change in the FRET distribution was detected upon addition of 50 nM WRN.

(c) FRET histograms for the G4 (10 nt) substrate, with a 10 nt ssDNA between the G4 motif and duplex region. No change in FRET distribution was observed following addition of 50 nM of RecQL5.

(d) FRET histograms for the G4 (10 nt) substrate, with a 10 nt ssDNA between the G4 motif and duplex region. No change in FRET distribution was observed following addition of 50 nM of Pif1.

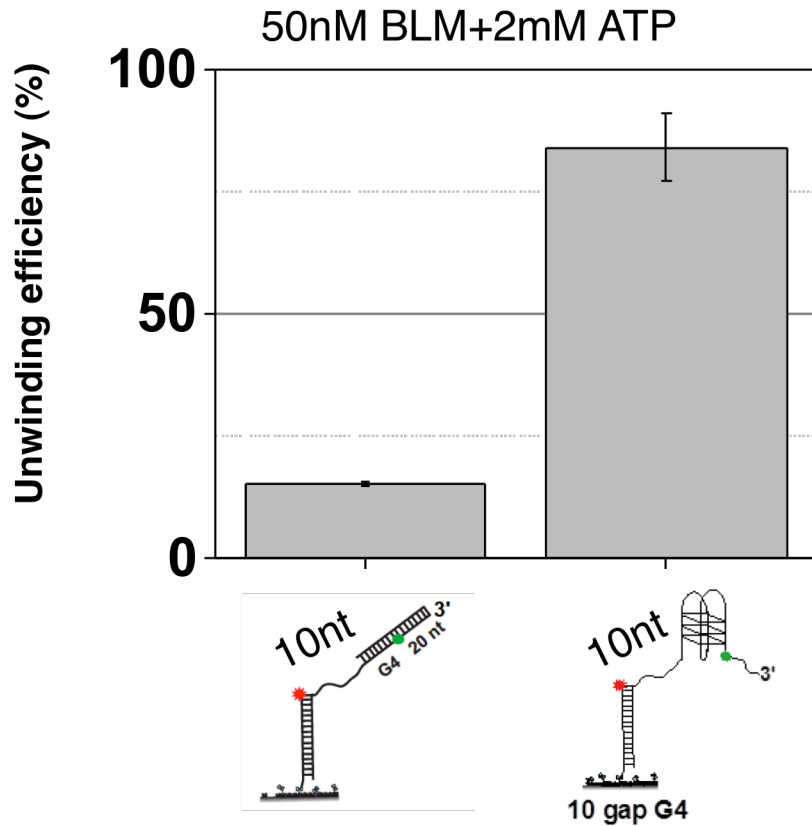
Histograms were generated after subtracting the zero FRET values and truncating the photobleached part from FRET trajectory. A minimum of 100 smFRET trajectories was used to generate the histograms. The concentration of K^+ was kept at 50 mM.



Supplementary Figure 8. Unwinding yields of BLM for c-kit substrates and G4 substrates having mixed sequence spacer.

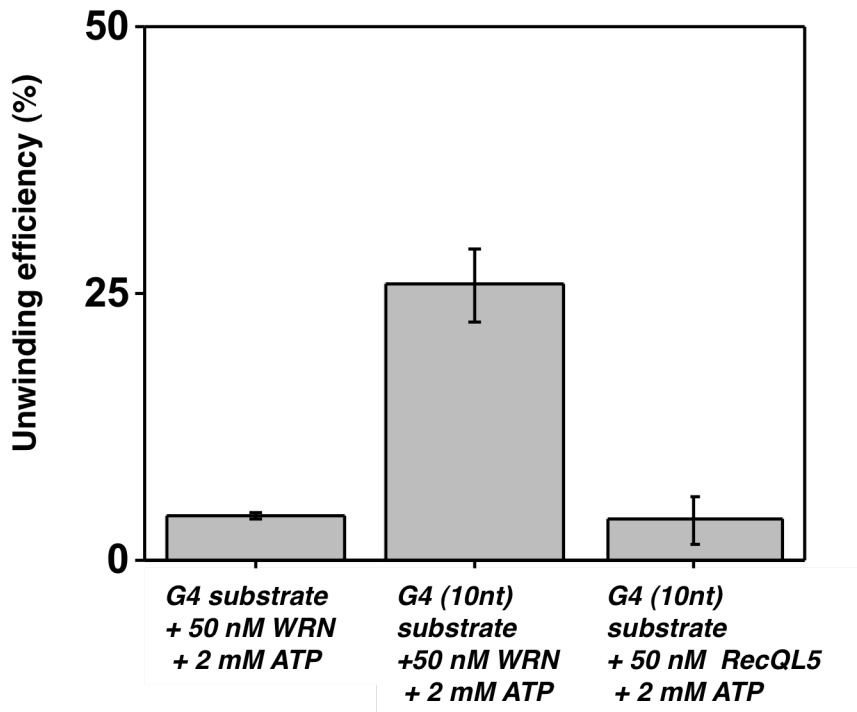
(a) Quantification of BLM unwinding efficiency at 50 nM BLM and 2 mM ATP for the c-kit2 G4 substrate and c-kit2 G4 (10 nt) substrate, showing efficient unwinding in the latter.

(b) Quantification of BLM unwinding efficiency at 50 nM BLM and 2 mM ATP for the G4 substrate, G4 (5nt) substrate with a mixed sequence ssDNA spacer, and G4 (5 nt) substrate with a mixed sequence ssDNA spacer. Unwinding was observed only for the substrates containing the ssDNA spacers. (Error bar = S.E.M. n=5)



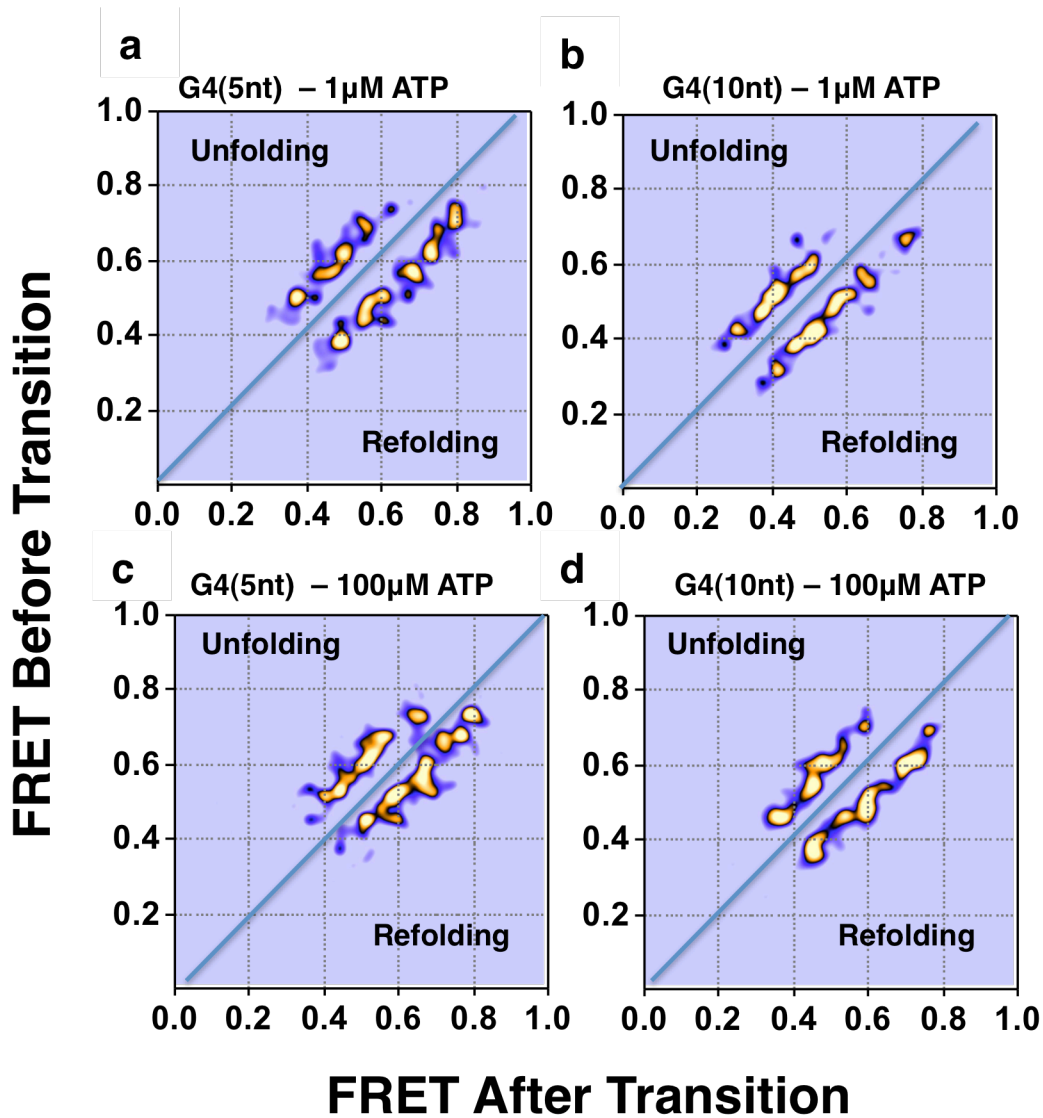
Supplementary Figure 9. Comparison of BLM's unwinding yields in the G4 (10nt) substrate and in 10 nt gapped substrate.

Quantification of BLM unwinding efficiency at 50 nM BLM and 2 mM ATP for the G4 (10 nt) substrate and a 10 nt gapped duplex substrate. (Error bar = S.E.M. n=4)



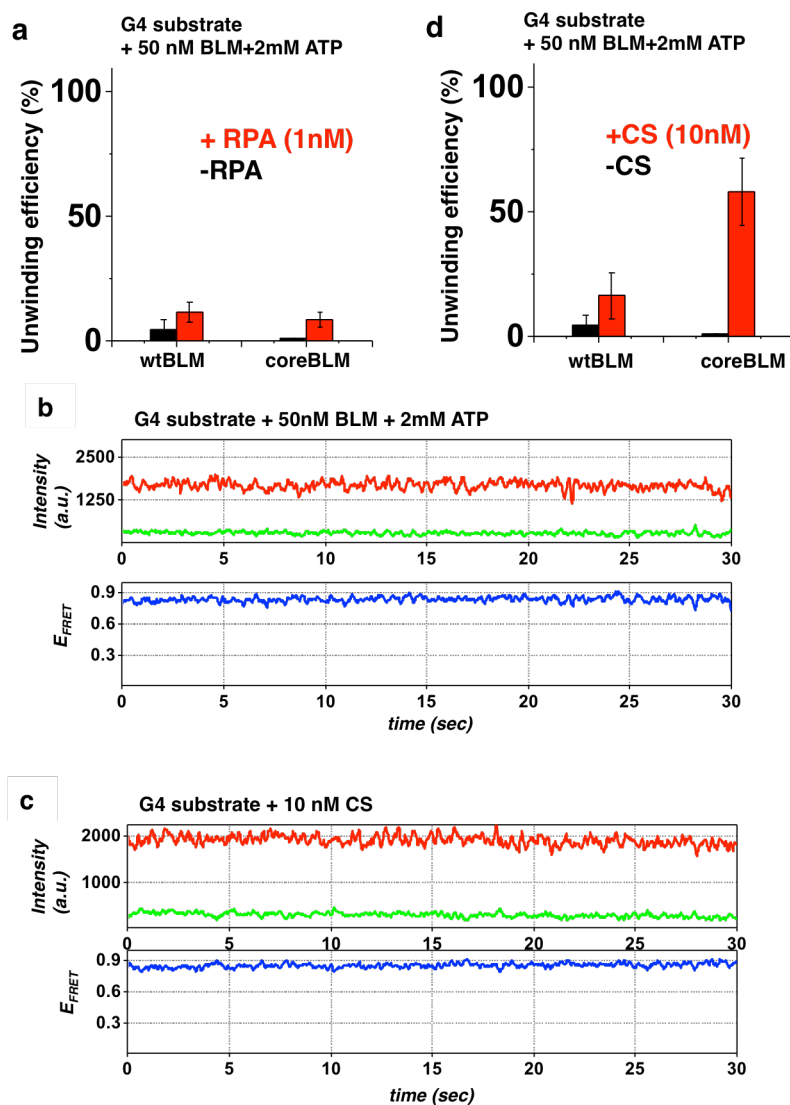
Supplementary Figure 10 | Unwinding yields of WRN and RecQL5 in a gapped substrate.

Quantification of WRN unwinding efficiency at 50 nM WRN and 2 mM ATP for the G4 and G4(10 nt) substrate are shown in the first and second columns, respectively. Unwinding by WRN was observed for the G4 (10 nt) substrate, but not for the G4 substrate. We note the WRN generally exhibit poor unwinding activity as compared with BLM even 3' tailed substrates. The last column shows that no unwinding was observed for RecQL5 (50 nM RecQL5 and 2 mM ATP) in the G4 (10 nt) substrate. (Error bar = S.E.M. n=4)



Supplementary Figure 11 | TDP for two substrates at different ATP concentrations.

(a-d) Generated TDP matrix for each G4 (5 nt) and G4 (10 nt) substrates in the presence of 50 nM BLM and 1 μ M or 100 μ M ATP. The color intensity corresponds to transition probability. The y-axis is the initial FRET prior to transition, and the x-axis is the final FRET after transition. (a) G4 (5nt) substrate and 1 μ M ATP. (b) G4 (10nt) substrate and 1 μ M ATP. (c) G4 (5nt) substrate and 100 μ M ATP. (d) G4 (10nt) substrate and 100 μ M ATP. Peaks corresponding to unfolding (above diagonal) and refolding (below diagonal) transitions of the G4 motif.

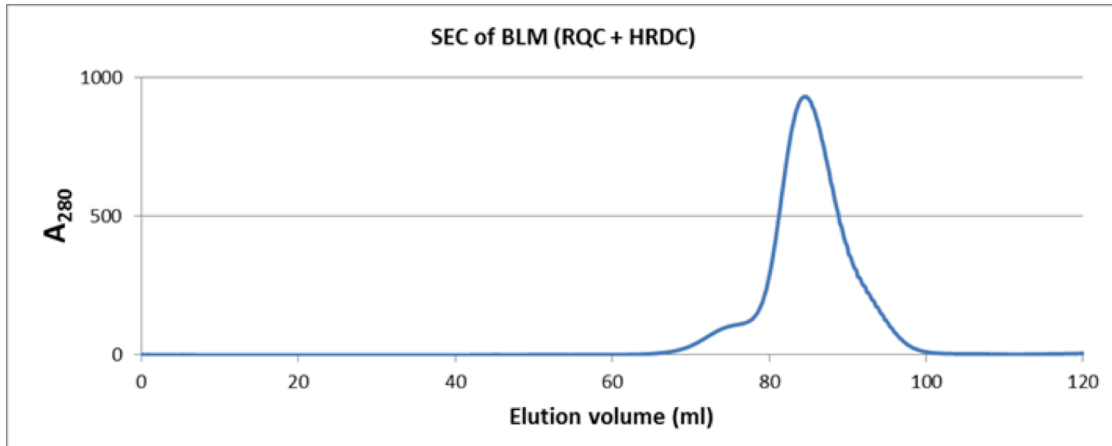


Supplementary Figure 12 | Effect of RPA and CS in the presence of coreBLM and wtBLM.

(a) Quantification of core BLM and wtBLM unwinding efficiency of the G4 substrate at 50 nM BLM and 2 mM ATP, either alone or with 1nM RPA. (Error bar = S.E.M. n=4)

(b/c) Representative smFRET trajectories of the G4 substrate in the presence of (b) 50 nM BLM + 2mM ATP showing persistent high FRET. (c) 10 nM CS showing persistent high FRET.

(d) Quantification of core BLM and wtBLM unwinding efficiency of the G4 substrate at 50 nM BLM and 2 mM ATP, either alone or with 10 nM CS. (Error bar = S.E.M. n=5)



Supplementary Figure 13 | Gel filtration absorptions profile of the RQC-HRDC fragment.

The RQC-HRDC fragment migrates as a single peak in the gel filtration absorption profile.

Supplementary Table 1: DNA oligos used in this study.

No.	Name	Sequence
1	Biotin – duplex top	5'-/Cy5/GCC TCG CTG CCG TCG CCA/3BioTEG/-3'
2	Telomeric G4 substrate strand	5'-TGG CGA CGG CAG CGA GGC G GGT TAG GGT TAG GGT TAG GG/iCy3/TTT TTT TTT TTT TTT TT-3'
3	Telomeric G4(5nt) substrate strand	5'-TGG CGA CGG CAG CGA GGC TTT TTG GGT TAG GGT TAG GGT TAG GG/iCy3/T TTT TTT TTT TTT TTT T-3'
4	Telomeric G4(10nt) substrate strand	5'-TGG CGA CGG CAG CGA GGC TTT TTT TTT TG GGT TAG GGT TAG GGT TAG GG/iCy3/T TTT TTT TTT TTT TTT TTT T-3'
5	Telomeric G4 complementary strand (CS)	5'-CCC TAA CCC TAA CCC TAA CCC-3'
6	T10 tailed unwinding substrate strand	5'-TGG CGA CGG CAG CGA GGC TTTTTTTTTT /3Cy3Sp/3'
7	Complement strand of Telomeric G4 and T20 tail	5'-AAA AAA AAA AAA AAA AAC CCT AAC CCT AAC CCT AAC CC-3'
8	T30 tailed unwinding substrate strand	5'-TGG CGA CGG CAG CGA GGC TTT TTT T/iCy3/TTT TTT TTT TTT TTT TTT TT-3'
9	Non complementary strand	5'-AGG CGA CGG CAG CGA GGC-3'
10	Hairpin unwinding substrate strand	5'- TGG CGA CGG CAG CGA GGC GCG AGC GGC ATC TTT GAT GCC GCT CGC TTT /iCy3/TTT TTT TTT TTT TT -3'
11	Telomeric G4 substrate strand, 7 nt tail	5'-TGG CGA CGG CAG CGA GGC G GGT TAG GGT TAG GGT TAG GG/iCy3/TTT TTT T-3'
12	c-kit2 G4 substrate	5'- TGG CGA CGG CAG CGA GGC CGG GCG GGC GCG AGG GAG GGG /iCy3/TTT TTT TTT TTT TTT TT -3'
13	c-kit2 G4 substrate (10nt) spacer	5'- TGG CGA CGG CAG CGA GGC TTT TTT TTT TCG GGC GGG CGC GAG GGA GGG G/iCy3/TT TTT TTT TTT TTT TTT -3'
14	Telomeric G4(5nt) mixed base spacer	5'- TGG CGA CGG CAG CGA GGC ACG GCG GGT TAG GGT TAG GGT TAG GG/iCy3/T TTT TTT TTT TTT TTT T -3'
15	Telomeric G4(10nt) mixed base spacer	5'- TGG CGA CGG CAG CGA GGC ACG ATC TGG CGG GTT AGG GTT AGG GTT AGG G/iCy3/TT TTT TTT TTT TTT TTT TTT -3'